Published in final edited form as:
Dev Cell. 2012 August 14; 23(2): 280–291. doi:10.1016/j.devcel.2012.06.006.

Tbx5-Hedgehog Molecular Networks Are Essential in the Second Heart Field for Atrial Septation

Linglin Xie[1], **Andrew D. Hoffmann**[1], **Ozanna Burnicka-Turek**[1], **Joshua M. Friedland-Little**[1], **Ke Zhang**[2], and **Ivan P. Moskowitz**[1,*]

[1]Departments of Pediatrics and Pathology, The University of Chicago, Chicago, IL 60637, USA

[2]Department of Pathology, The University of North Dakota, Grand Forks, ND 58202, USA

Abstract

Summary—The developmental mechanisms underlying human congenital heart disease (CHD) are poorly understood. Atrial septal defects (ASDs) can result from haploinsufficiency of cardiogenic transcription factors including TBX5. We demonstrated that *Tbx5* is required in the second heart field (SHF) for atrial septation in mice. Conditional *Tbx5* haploinsufficiency in the SHF but not the myocardium or endocardium caused ASDs. *Tbx5* SHF knockout embryos lacked atrial septum progenitors. We found that *Tbx5* mutant SHF progenitors demonstrated cell-cycle progression defects and that *Tbx5* regulated cell-cycle progression genes including *Cdk6*. Activated *hedgehog (Hh)* signaling rescued ASDs in *Tbx5* mutant embryos, placing *Tbx5* upstream or parallel to *Hh* in cardiac progenitors. *Tbx5* regulated SHF *Gas1* and *Osr1* expression, supporting both pathways. These results describe a SHF *Tbx5-Hh* network required for atrial septation. A paradigm defining molecular requirements in SHF cardiac progenitors for cardiac septum morphogenesis has implications for the ontogeny of CHD.

Introduction

Current understanding of the transcriptional regulation of cardiac development (reviewed in Olson, 2006) has yet to illuminate the molecular ontogeny of congenital heart disease (CHD). Longstanding genetic studies have implicated dominant mutations in transcription factor genes TBX5, NKX2-5, and GATA4 in human congenital atrial septal defects (ASDs) (Basson et al., 1997; Garg et al., 2003; Li et al., 1997; Schott et al., 1998), a common form of CHD. Elegant work has demonstrated that these transcription factors are expressed in the atrium during atrial septation, physically interact to form a macromolecular complex, and combinatorially activate atrial gene expression (Bruneau et al., 2001; Garg et al., 2003; Hiroi et al., 2001; Takeuchi and Bruneau, 2009). These observations support an intra-cardiac paradigm for atrial septation in which normal intracardiac transcription factor dose is essential for morphogenesis of the atrial septum. However, the molecular and developmental mechanisms describing how reduced cardiac transcription factor dose caused ASDs remain unknown.

Haploinsufficiency of TBX5 causes Holt-Oram syndrome, characterized by structural cardiac and limb abnormalities (Basson et al., 1997; Li et al., 1997). The majority of patients have cardiac defects and ASDs are the most common, accounting for approximately half (Bruneau et al., 1999). In a well-established *Tbx5* mouse model, 40% of mice

*Correspondence: imoskowitz@uchicago.edu.

Supplemental Information: Supplemental Information includes one figure and two tables and can be found with this article online at http://dx.doi.org/10.1016/j.devcel.2012.06.006.

haploinsufficient for *Tbx5* demonstrated ASDs (Bruneau et al., 2001). Several *Tbx5* target genes have been identified, including *Gja1*, *Gja5*, and *Nppa*, but none appear to regulate the development of the atrial septum (Bruneau, 2003; Bruneau et al., 2001; Garg et al., 2003). Thus, the pathogenesis of cardiac structural abnormalities resulting from *Tbx5* haploinsufficiency remains unclear.

The developmental basis of atrial septum formation and ASD ontogeny has undergone significant recent revision. ASDs occur in different structural variants including secundum ASDs, in the region of the primary atrial septum (PAS), and primum ASDs, a type of atrioventricular septal defect (AVSD) in the region of the dorsal mesenchymal protrusion (DMP) (Anderson et al., 2003). Recent work has underscored the importance of the DMP in atrial and atrioventricular septation. Prior to formal atrial septation, the developing DMP is extracardiac mesenchyme associated with the dorsal mesocardium at the venous pole of the heart (∼E9–10 in the mouse). The DMP protrudes into the dorsal aspect of the atrial cavity, remains continuous with the primary atrial septum, and resides as a prominent structure in the posterior aspect of the mature atrioventricular mesenchymal complex at the completion of atrial septation (Snarr et al., 2007a). Recent work has correlated the deficiency of the DMP with primum ASDs, including the septal defects commonly associated with Down syndrome (Blom et al., 2003; Goddeeris et al., 2008; Hoffmann et al., 2009; Mommersteeg et al., 2006; Snarr et al., 2007b; Wessels et al., 2000). The DMP is marked by second heart field (SHF) markers *Mef2c-Cre* (Goddeeris et al., 2008) and *Isl1-Cre* (Snarr et al., 2007b) and is generated by a *Hedgehog* (*Hh*)-receiving lineage (Hoffmann et al., 2009). SHF *Hh*-signaling is required for atrial septation (Goddeeris et al., 2008; Hoffmann et al., 2009) and posterior SHF (pSHF) cardiac progenitors receiving *Hh*-signaling generate the atrial septum specifically (Hoffmann et al., 2009). These observations engender a working hypothesis that specification of a subset of pSHF progenitor cells specific for the atrial septum is a driver of the atrial septum morphogenesis days later in the heart proper.

We have implicated *Tbx5* in the pSHF upstream and parallel to *Hh*-signaling in atrial septation. We show that although myocardial or endocardial *Tbx5* haploinsufficiency had no structural consequences, SHF *Tbx5* haploinsufficiency recapitulated the ASDs caused by germline *Tbx5* haploinsufficiency. SHF *Tbx5* knockout caused a failure of DMP formation. *Tbx5* was required for cell-cycle progression of pSHF atrial septum progenitors. Remarkably, ASDs in *Tbx5* mutant embryos were rescued by constitutive *Hh*-signaling in atrial progenitors. We identified *Tbx5*-responsive loci *Gas1*, required for normal *Hh*-signaling, and *Osr1*, required for atrial septation, as *Tbx5* targets. These results place *Tbx5* upstream of and parallel to *Hh*-signaling in SHF atrial septum progenitors required for atrial septation and provide molecular support for a recent paradigm describing inflow tract CHDs as the result of SHF defects.

Results

Tbx5 Is Expressed in the Posterior SHF Including Gli1-Expressing Cells

Cardiac expression of *Tbx5* is well documented in mice from E8 into adulthood, although its expression in the SHF has not been examined in detail (Bruneau et al., 1999; Li et al., 1997). We evaluated *Tbx5* expression in the SHF at E9 and E10 (Figure 1). Strong *Tbx5* expression was observed in the posterior SHF (pSHF), DMP, and dorsal mesocardium surrounding the DMP at E9 (Figures 1A and 1C). *Tbx5* expression was observed in the pSHF, dorsal mesocardium, and the primary atrial septum (PAS) at E10 (Figures 1E and 1G). *Tbx5* was expressed bilaterally in the SHF but extended more dorsally on the right side than the left side (Figure 1G). Consistent with previous reports, strong *Tbx5* expression was also observed in the atria and the left ventricle (Bruneau et al., 1999). Expression of *Gli1*, a member of the *Gli* transcription factor family responsible for *Hh* signal transduction and a

marker of *Hedgehog*-receiving atrial septum progenitors (Hoffmann et al., 2009), was observed in a bilaterally symmetric pattern that overlapped with *Tbx5* expression ventrally in the pSHF.

Tbx5 Is Not Required in the Myocardium or Endocardium for Atrial Septation

We hypothesized that *Tbx5* may be required in the SHF for atrial septation, not within the heart. We tested this hypothesis by analyzing mice haploinsufficient for *Tbx5* in the germline, myocardium, endocardium, or SHF. We observed primum ASDs in 40% of *Tbx5* germline haploinsufficient ($Tbx5^{-/+}$) embryos in a mixed genetic background (5/12) at E13.5, when atrial septation is normally complete (Figures 2K–2N), consistent with previously published results (Bruneau et al., 2001). The pulmonary veins appeared structurally normal in each case. We tested whether *Tbx5* was required for atrial septation in the myocardium using *Tnt:Cre* (Jiao et al., 2003), which drives *Cre* expression throughout differentiated cardiac myocardium by E9.5 (Jiao et al., 2003), to knock out a single loxP-flanked conditional allele of *Tbx5* ($Tbx5^{fl/+}$) (Bruneau et al., 2001) (Figures 2A–2D). A recombined *Tbx5* null allele was observed in heart tissue from $Tbx5^{Tnt\text{-}Cre/+}$ embryos by E9.5 (Figure 2I). Normal atrial septation was observed in all $Tbx5^{Tnt\text{-}Cre/+}$ (7/7) and littermate control $Tbx5^{fl/+}$ embryos (7/7) at E13.5 ($p = 1$) (Figure 2C versus 2D). $Tbx5^{Tnt\text{-}Cre/+}$ mutant embryos demonstrated thinner compact ventricular myocardium (Figure 2A versus 2B), consistent with the known requirement for *Tbx5* in myocardial proliferation (Goetz et al., 2006; Hatcher et al., 2001). We tested whether *Tbx5* was required for atrial septation in endocardium by analyzing mice haploinsufficient for *Tbx5* in the endocardium using *Tie2:Cre* (Kisanuki et al., 2001), which drives *Cre* expression throughout vascular endothelium including endocardial cushion endocardium by E9.5. A recombined *Tbx5* null allele was observed in hearts from $Tbx5^{Tie\text{-}Cre/+}$ embryos by E9.5 (Figure 2J). Normal atrial septation was observed in all $Tbx5^{Tie2\text{-}Cre/+}$ mutant embryos (7/7) and littermate control $Tbx5^{fl/+}$ embryos (7/7) at E13.5 ($p = 1$) (Figure 2G versus 2H), consistent with previous reports (Nadeau et al., 2010). These results demonstrated that *Tbx5* haploinsufficiency in myocardium or endocardium supported normal atrial septation.

Tbx5 Is Required in the SHF for Atrial Septation

We predicted that the dominant requirement for *Tbx5* in atrial septation might occur in SHF cardiac progenitors. We previously identified pSHF atrial septum progenitors as *Hh*-receiving cells, defined by $Gli1^{Cre\text{-}ERT2/+}$ expression (Hoffmann et al., 2009). We evaluated atrial septation in embryos conditionally haploinsufficient for *Tbx5* in the pSHF using $Gli1^{Cre\text{-}ERT2}$. $Tbx5^{Gli1Cre\text{-}ERT2/+}$ embryos and their littermate controls were administered tamoxifen to activate Cre-ERT2 at E7.5 and E8.5. ASDs were observed in 40% (5/12) of $Tbx5^{Gli1CreE\text{-}RT2/+}$ embryos but no littermate control $Tbx5^{fl/+}$ embryos at E13.5 (0/7; $p = 0.0466$) (Table 1; Figures 2O–2R). Because $Gli1^{CreERT2}$ is a knockin allele, it was formally possible that the ASDs were caused by a combined deficiency of *Tbx5* and *Hh-signaling*, not *Tbx5* haploinsufficiency alone. Therefore, we directly tested for a genetic interaction between *Tbx5* and *Gli1* in atrial septation by analyzing $Tbx5^{-/+}$; $Gli1^{Cre\text{-}ERT2/+}$ embryos. ASD incidence was no different in $Tbx5^{-/+}$ versus $Tbx5^{-/+}$; $Gli1^{Cre\text{-}ERT2/+}$ embryos (5/12 versus 5/11; $p = 0.8547$) and no new cardiac defects were observed in compound heterozygotes, suggesting that presence of the *Gli1* knockin allele had no discernible effect on the incidence or expression of phenotypes caused by *Tbx5* haploinsufficiency (Table 1). Nonetheless, these results implicate either *Tbx5* alone or *Tbx5* with *Hh* signaling in atrial septum progenitors. Together with the exclusion of the requirement for *Tbx5* from the myocardium and endocardium, these results place the requirement for *Tbx5* in atrial septation in the SHF.

Tbx5 Is Essential for DMP Development

To examine the cellular mechanism by which *Tbx5* haploinsufficiency caused ASDs, we performed genetic inducible fate mapping (GIFM) of atrial septum progenitors in *Tbx5* germline heterozygotes. PSHF atrial septum progenitors were marked by $Gli1^{CreERT2/+}$ expression in combination with the *Cre*-dependent *lacZ* reporter allele *R26R* (Soriano, 1999). The effect of *Tbx5* haploinsufficiency on the number and distribution of the marked atrial septum progenitors was analyzed in $Tbx5^{-/+}$; $R26R^{Gli1Cre\text{-}ERT2/+}$ mutant and compared to $R26R^{Gli1Cre\text{-}ERT2/+}$ littermate controls. β-galactosidase-expression was induced by tamoxifen administration at E7.5 and E8.5 and descendants of marked atrial septum progenitors were analyzed at E10.5 in the DMP. A hypoplastic DMP was observed in $Tbx5^{-/+}$; $R26R^{Gli1Cre\text{-}ERT2}$ embryos (Figures 3A and 3C versus Figures 3B and 3D). β-galactosidase-positive cells were decreased by 50% in the DMP of *Tbx5* mutant embryos (187.4 ±11.5 versus 92.4 ± 24.1, p = 0.0265) (Figure 3E). Thus, *Tbx5* haploinsufficiency caused a decrease in the number of cells generated by the pSHF atrial septum progenitor lineage.

We next analyzed the requirement for *Tbx5* in SHF cardiac progenitors. We created conditional SHF *Tbx5* knockouts using two SHF *Cre* lines, *Mef2c:Cre* (Verzi et al., 2005) and *Gli1:Cre-ERT2*. In $Tbx5^{Mef2c\text{-}Cre}$ embryos, *Tbx5* expression was abolished in the pSHF and DMP (Figures 3G and 3I versus Figures 3F and 3H, black arrow) but maintained in the atrial and ventricular wall (Figures 3F and 3G, red arrowhead). The DMP was absent or extremely hypoplastic in all $Tbx5^{Mef2c\text{-}Cre}$ embryos (5/5) compared to littermate $Tbx5^{fl/fl}$ controls (0/7; p = 0.0005) at E10.5 (Table 1; Figures 3J and 3L versus Figures 3K and 3M). We analyzed the effect of SHF *Tbx5* knockout on the SHF fate map and found that *Tbx5* is absolutely required for the pSHF lineage as defined by *Mef2c:Cre* expression: β-galactosidase-expressing cells were entirely absent from the DMP region of $Tbx5^{Mef2c\text{-}Cre}$ embryos at E9.5 (Figures 3Q versus 3P). ASDs were also observed in all $Tbx5^{Gli1Cre\text{-}ERT2}$ embryos at E10.5 (Table 1) (5/5; p = 0.0005 versus $Tbx5^{fl/fl}$). These results demonstrate a requirement for *Tbx5* in development of the DMP utilizing two independent SHF *Cre*-drivers.

Tbx5 Is Required for Proliferation of Atrial Septum Progenitors

Plausible mechanisms for absence of the pSHF lineage in *Tbx5* mutants included altered proliferation or apoptosis; we therefore assessed both in *Tbx5* mutant embryos. Proliferation was assessed in wild-type and $Tbx5^{-/+}$ embryos by counting BrdU incorporated cells in the pSHF and DMP at E9.5. We found 44% less BrdU-positive SHF cells in $Tbx5^{-/+}$ embryos than in wild-type control embryos (Figures 4A–4E, 61.4% ± 4.3% versus 34% ± 5.7%, p = 0.001). We next assessed the requirement for *Tbx5* specifically in atrial septum progenitors by combining GIFM (Joyner and Zervas, 2006) with conditional SHF *Tbx5* knockout. Dual BrdU/β-*galactosidase* positive cells, indicative of proliferating atrial septum progenitors, were much more frequent in $R26R^{Gli1Cre\text{-}ERT2/+}$ control embryos than in $Tbx5^{Gli1Cre\text{-}ERT2}$; $R26R^{Gli1Cre\text{-}ERT2/+}$ mutant embryos (Figure 4F, 34.9% ± 8.4% versus 21.6% ± 5.6%, p = 0.0492). No apoptosis was observed in *Hh*-receiving cells within the pSHF of either $Tbx5^{Gli1Cre\text{-}ERT2}$; $R26R^{Gli1Cre\text{-}ERT2/+}$ *or* $R26R^{Gli1Cre\text{-}ERT2/+}$ littermate control embryos as analyzed by TUNNEL staining (Figure S1 available online). Together, these findings define a requirement for *Tbx5* in proliferation but not survival of pSHF cardiac progenitors.

Distinct *Tbx5*-Dependent Transcripts in the SHF and the Heart

To identify *Tbx5*-dependent molecular networks required for atrial septation, we compared the pSHF transcriptomes of wild-type and $Tbx5^{-/+}$ mutant embryos. We microdissected the heart, pSHF, and anterior SHF (aSHF) from E9.5 embryos and molecularly verified our

dissections by real-time PCR. We observed a 35.8-fold higher *Tbx5* expression in the pSHF versus the aSHF, consistent with the selective expression of *Tbx5* in the pSHF (Figures 1A and 1C). Transcriptional profiling of pSHF samples was performed on Agilent Mouse Whole Genome Arrays (n = 4 WT pools and 4 $Tbx5^{-/+}$ pools). The R statistical package SAM was used to detect differentially expressed genes (Tusher et al., 2001) and revealed upregulation of 343 genes and downregulation of 672 genes with >2-fold changes and false discovery rates <5% in $Tbx5^{-/+}$ versus control pSHF (Table S1). Real-time PCR for 55 selected transcripts confirmed significant expression changes in 47 genes (87%; Figure 5 and data not shown). *Tbx5* expression was ∼50% reduced in both the heart and pSHF of *Tbx5* heterozygotes, as expected (Figures 4G and 4H). Expression of *Gja5* and *Nppa*, previously identified *Tbx5* downstream targets in the heart (Bruneau et al., 2001; Mori et al., 2006), were significantly decreased in the heart, but not in the pSHF. Expression of *Gata6* and *Mef2c* were significantly decreased in the pSHF, but not in the heart at E9.5 (Figures 4G and 4H). These results suggested that pSHF and heart *Tbx5*-dependent transcriptomes might be distinct.

Repression of interphase mitotic cell cycle, mitotic sister chromatid segregation, and G1-S transition of mitotic cell cycle were identified by gene set enrichment analysis (GSEA) (Efron and Tibshirani, 2001) of *Tbx5*-dependent transcripts. Transcriptional profiling identified 14 differentially expressed cell-cycle genes and each was verified by real-time PCR (Figures 4I and 4J). *Cdk2*, *Cdk6*, *Cdk8*, *Cdc25a*, *PCNA*, and *Tfdp2*, promoters of the G1 to S transition (Malumbres and Barbacid, 2005; Xiong et al., 1992), were downregulated whereas *Cdkn2a*, a repressor of G1 to S transition (Chan et al., 1995), was upregulated in the $Tbx5^{-/+}$ pSHF (Figure 4I). *Cdca2*, *Cdc26*, *Cdc27*, *Cdk5rap*, *Anapc1*, *Anapc10*, and *Cenpe* all regulate M to G1 phase transition (Dong et al., 2007; Barr et al., 2010; Pérez-Pérez et al., 2008; Rao et al., 2009; Vagnarelli et al., 2006; Wehman et al., 2007) and were misexpressed in the $Tbx5^{-/+}$ pSHF transcriptome (Figure 4J). These results demonstrated that *Tbx5* is required for normal transcriptional control of genes required for cell-cycle progression in the pSHF, and suggested that a pSHF cell cycle defect in *Tbx5* mutant embryos may mechanistically underlie the observed ASDs.

Tbx5 Controls Cell-Cycle Progression of Atrial Septum Progenitors

We tested the hypothesis that *Tbx5* regulates pSHF cell-cycle progression by analyzing phosphorylated-Ser10-H3-histone (H3S10) immunohistochemistry, which differentially marks mitotic cells in G2 and M phase (Crosio et al., 2002): punctate in G2 phase (Figures 4M–4Mm′ and 4N–4Nn′, red arrowhead) and homogeneous in M phase (Figures 4M and 4N, white arrowhead). We observed 44% fewer mitotic cells in the mutant $Tbx5^{Gli1Cre\text{-}ERT2}$; $R26R^{Gli1Cre\text{-}ERT2/+}$ pSHF than the control $R26R^{Gli1Cre\text{-}ERT2/+}$ pSHF (7.73 ± 0.51% versus 4.25 ± 0.71%, p = 0.0037; Figures 4N and 4P versus 4M and 4O). There was no difference in the number of cells in G2 phase (12.03 ± 1.68% versus 10.03 ± 1.25%; p = 0.8744). We concluded that *Tbx5* is required for pSHF mitotic cell-cycle progress.

We hypothesized that *Tbx5* may promote cell-cycle progress by directly regulating cell-cycle component transcription. *Cdk6*, a cyclin-dependent kinase, was identified as a candidate based on its *Tbx5*-dependent pSHF expression (Figure 4I). We used the overlap of evolutionary conservation and *Tbx5* binding sites from ChIP-seq studies in the HL-1 cardiomyocyte cell line (He et al., 2011) to identify a conserved canonical *Tbx5* binding site (Table S2) in proximity to the *Cdk6* promoter (Figure 4R). *Tbx5* transactivated luciferase expression from a *Cdk6* genomic fragment containing this site 10-fold compared to vector alone (p = 0.009) (Figure S4; Table S2). This result suggests that *Tbx5* promotes pSHF proliferation by directly regulating cell-cycle gene transcription.

Hh-Signaling Rescues Atrial Septation in *Tbx5* SHF Mutant Embryos

The requirement for *Tbx5* in *Hh*-receiving cells (Figure 3) suggested that *Tbx5* and *Hh*-signaling might interact in atrial septum progenitor specification. We tested this hypothesis by analyzing an intercross between $Tbx5^{-/+}$ and $Smo^{-/+}$, encoding the obligate *Hh* receptor. $Smo^{-/+}$ mice have quantitatively depressed *Hh*-signaling, but do not have structural cardiac defects (Zhang et al., 2001). We observed a significant increase in ASD incidence in $Smo^{-/+}$; $Tbx5^{-/+}$ double heterozygotes (7/8) (Table 1; Figures 5A–5D) compared to either $Tbx5^{-/+}$ (5/12; p = 0.0404) or $Smo^{-/+}$ (0/7; p = 0.0005) (Figures 5A and 5C) single heterozygotes at E14.5.

To elucidate the hierarchy between *Tbx5* and *Hh*-signaling, we performed epistasis analysis. We combined conditional *Tbx5* SHF haploinsufficiency or knockout with conditional SHF activation of *Hh*-signaling by *Cre*-dependent expression of *SmoM2*, a constitutively activated *Smo* mutant (Mao et al., 2006). In control *R26-SmoM2*$^{Gli1Cre\text{-}ERT2/+}$ embryos, normal septation was observed at E14.5 (10/10) (Figures 5F and 5H). Constitutive *Hh*-signaling rescued atrial septation in conditional SHF *Tbx5* heterozygotes: ASDs were observed in 0% of $Tbx5^{Gli1Cre\text{-}ERT2/+}$; *R26-SmoM2*$^{Gli1Cre\text{-}ERT2/+}$ embryos (0/11) in contrast to 40% of $Tbx5^{Gli1Cre\text{-}ERT2/+}$ embryos (5/12, p = 0.01) (Table 1; Figures 5J and 5L versus Figures 5I and 5K). Remarkably, constitutive *Hh*-signaling rescued atrial septation in *Tbx5* SHF knockout embryos. ASDs were observed in only 20% of $Tbx5^{Gli1Cre\text{-}ERT2}$; *R26-SmoM2*$^{Gli1Cre\text{-}ERT2/+}$ embryos (1/5) in contrast to 100% of $Tbx5^{Gli1Cre\text{-}ERT}$ embryos (5/5; p value = 0.01) (Figures 5N and 5P versus Figures 5M and 5O). The observation that *Hh*-signaling can rescue atrial septation in *Tbx5* SHF knockout embryos suggested that *Tbx5* acts upstream or in parallel to *Hh*- signaling in SHF atrial septum progenitors.

We hypothesized that *Hh*-signaling may rescue atrial septation by correcting the cell-cycle defect in *Tbx5* mutant embryos. We analyzed atrial septum progenitor cell-cycle progression in the presence and absence of constitutive *Hh*-signaling in *Tbx5* mutant embryos. We quantitated M phase H3S10 positive cells in 800 SHF atrial septum progenitors at E9.5 in each genotype. There was no significant difference in the number of H3S10 positive cells in the structurally normal *Smo-M2*$^{Gli1Cre\text{-}ERT2/+}$ (5.71 ± 0.54%) compared to control *Gli1Cre*$^{ERT2/+}$ embryos (6.16 ± 0.75%, p = 0.63) (Figure 5Q). In contrast, a significant proliferation defect was observed in mutant $Tbx5^{Gli1Cre\text{-}ERT2}$ embryos (4.21% ± 0.15%), as expected (Figure 4). The proliferation decrement observed in *Tbx5* mutants was rescued in $Tbx5^{Gli1Cre\text{-}ERT2}$; *Smo-M2*$^{Gli1Cre\text{-}ERT2/+}$ embryos (5.66% ± 0.23%, p = 0.017). The number of H3S10 positive atrial septum progenitors in $Tbx5^{Gli1Cre\text{-}ERT2}$; *Smo-M2*$^{Gli1Cre\text{-}ERT2/+}$ embryos (5.66 ± 0.23%) was not different than that observed in control *Gli1Cre*$^{ERT2/+}$ embryos (6.16 ± 0.75%; p = 0.274) (Figure 5Q). These results suggest that activated *Hh*-signaling rescues the morphologic defects in *Tbx5* mutant embryos by a mechanism that includes normalization of cell proliferation.

Tbx5 Acts Upstream and Parallel to *Hh*-Signaling in the SHF

We sought molecular evidence for the SHF *Tbx5-Hh*-signaling hierarchy. If *Tbx5* acted upstream of *Hh*-signaling, we predicted that quantitative markers for *Hh*-signaling would be decreased in *Tbx5* mutants. To assess the integrity of *Hh*-signaling, we quantitatively evaluated *Hh*-dependent transcripts *Patched1* (*Ptch1*), the primary *Hh* membrane receptor, and *Gli1*. *Ptch1* and *Gli1* expression were both significantly reduced in the pSHF of $Tbx5^{Mef2c\text{-}cre}$ mutant embryos by real-time PCR (Figure 6A), consistent with a requirement for *Tbx5* upstream of *Hh*-signaling. We hypothesized that *Tbx5* may directly regulate *Hh*-signaling components and examined the expression of the known *Hh*-signaling pathway members at or upstream of *Smo*, including *Smo*, *Boc*, *Gas1*, and *Cdo* (Allen et al., 2011; Izzi et al., 2011). We found that expression of *Gas1*, but not the other candidate genes, was

significantly decreased in the pSHF of *Tbx5*$^{Mef2c\text{-}Cre}$ mutant embryos (Figure 6A and data not shown). We hypothesized that *Gas1* may be a direct *Tbx5* target. We bioinformatically interrogated the *Gas1* locus to identify potential *Tbx5*-responsive elements, utilizing the overlap of evolutionary conservation and ChIP-seq studies identifying *Tbx5* binding sites in the atrial cardiomyocyte HL-1 cell line (He et al., 2011) and identified a conserved canonical *Tbx5* binding site (Table S2) in proximity to the *Gas1* promoter. We found that *Tbx5* significantly transactivated *luciferase* expression from a *Gas1* genomic region containing this site (Figure 6B; Table S2). Vector alone demonstrated no *Tbx5*-dependent activation in vitro (Figure 6B). Together, these results suggest that *Tbx5* potentates pSHF *Hh*-signaling by a mechanism that includes activation of *Gas1* expression. However, the *Tbx5* mutant phenotype could not be explained by the observed partial loss of *Hh*-signaling (Figure 6A), suggesting that *Tbx5* may act parallel to *Hh*-signaling in addition to hierarchically in the SHF.

We identified odd-skipped related-1 (*Osr1*), encoding a zinc finger transcription factor (Wang et al., 2005), as a candidate *Tbx5* and *Hh*-signaling target gene in the SHF required for atrial septation. *Osr1* mutant mice demonstrated absence of the atrial septum (Wang et al., 2005) and *Osr1* is upregulated in a *Tbx5* overexpression model (Plageman and Yutzey, 2006). We found that *Osr1* expression was significantly reduced in the pSHF of both *Tbx5*$^{-/+}$ *and Shh*$^{-/-}$ mutant embryos by real-time PCR at E9.5 (Figure 6H). We tested whether *Osr1* was a direct *Tbx5* target. We bioinformatically interrogated the *Osr1* locus to identify potential *Tbx5*-responsive elements using overlap of evolutionary conservation and previously identified *Tbx5* binding sites in the cardiomyocyte HL-1 cell line (He et al., 2011). We identified and cloned four distinct regions with *Tbx5* binding sites within 30 kb downstream of the *Osr1* gene (Osr1-F1-F4, Figure 6K); no other *Tbx5* binding sites were encountered for an additional 300 kb downstream or in the upstream intergenic region. We found that *Tbx5* significantly transactivated *luciferase* expression from two of the four *Osr1* cloned genomic regions, Osr1F1 and Osr1F4 (Figure 6I; Table S2), but not from the two other regions (Osr1F2 or Osr1F3) or vector alone (Figure 6I; Table S2). We next asked if *Tbx5* physically occupies the *Tbx5*-responsive *Osr1* genomic regions in the SHF in vivo during atrial septum progenitor specification. We performed ChIP-PCR for *Tbx5* from the pSHF at E10.5, microdissected from 50 wild-type embryos. ChIP-PCR demonstrated significant *Tbx5*-dependent enrichment for the Osr1F1 fragment, containing three canonical *Tbx5* binding sites (Figure 6J; Table S2), and the Osr1F4 fragment, containing a single canonical *Tbx5* binding site (Figure 6J; Table S2). These results identify *Osr1* as a direct downstream target of *Tbx5* in the SHF and establish a *Tbx5*-*Osr1* pathway parallel to *Hh*-signaling required for atrial septation.

Discussion

Tbx5 Is Required in the SHF: Implications for the Ontogeny of ASDs

In this study, we have demonstrated that the requirement for *Tbx5* in atrial septation lies in the pSHF. *Tbx5* was expressed robustly in the pSHF, in atrial septum progenitors marked by *Gli1* expression (Figure 1) (Hoffmann et al., 2009). Haploinsufficiency of *Tbx5* in *Hh*-receiving pSHF cells caused primum ASDs identical to those observed in *Tbx5*$^{-/+}$ embryos (Figure 2) and *Tbx5* knockout in the pSHF or atrial septum progenitors caused absence of the DMP, the structural anlage of the ventral atrial septum (Figure 3). This structural abnormality may have been caused by a proliferation defect of atrial progenitors, whose mitotic cell-cycle progress was impeded in *Tbx5* mutant embryos (Figure 4). Atrial septation in *Tbx5* mutant embryos was rescued by constitutive *Hh*-signaling, placing Tbx5 activity upstream or parallel to *Hh*-signaling. *Gas1* was identified as a *Tbx5* downstream target (Figures 5 and 6), providing evidence that *Tbx5* acts upstream of *Hh*-signaling in the SHF,

and *Osr1*, a zinc finger transcription factor required for atrial septation, was identified as a direct *Tbx5* target in the SHF. Taken together, these observations define *Hh*-dependent and parallel pathways regulated by *Tbx5* in SHF atrial septum progenitors required for atrial septation. This work strengthens the recent paradigm implicating SHF defects in the ontogeny of ASDs.

The question of where and when genes are required for cardiac morphogenesis has significant consequences for understanding CHD ontogeny. Although cardiogenic transcription factors implicated in ASDs have been assumed to be required in the myocardium, we demonstrate that *Tbx5* is required for atrial septation in SHF cardiac progenitors. Endocardial knockout of *Tbx5* can cause secundum ASDs (Nadeau et al., 2010). However, endocardial *Tbx5* haploinsufficiency supported normal atrial septation (Figure 2). Thus, the SHF is more sensitive to *Tbx5* dose than the endocardium, suggesting a more significant role for the SHF and more modest role for the endocardium in ASDs caused by dominant Tbx5 mutations. Elucidating a SHF role for *Tbx5* in atrial septation provides momentum to the paradigm describing the molecular events in SHF progenitors as organizers of atrial septation (e.g., Snarr et al., 2007b; Goddeeris et al., 2008; Hoffmann et al., 2009). We predict that the requirement for other genes implicated in human ASDs also resides in the SHF. For example, both *Nkx2-5* and *Gata4* are highly expressed in the SHF, particularly in the region overlapping *Hh*-receiving atrial septum progenitors in the pSHF and later within the DMP (Kasahara et al., 1998; Kuo et al., 1997; Ueyama et al., 2003). More generally, we speculate that molecular diversity generated early among cardiac progenitors is an organizer of structural cardiac morphogenesis that occurs many days later.

Distinct *Tbx5*-Dependent Pathways in the SHF and in the Heart

Our transcriptional profiling experiments provide evidence for distinct *Tbx5*-dependent molecular pathways in the heart and pSHF (Figure 4). Genes previously shown to be *Tbx5* targets in the heart, e.g., *Nppa* and *Gja5* (Mori et al., 2006), were independently identified in our profiling experiments (Figure 4). However, expression of these intracardiac *Tbx5* targets was unchanged by *Tbx5* dose in the pSHF (Figure 4). In contrast, a set of *Tbx5* downstream genes is revealed in the pSHF, including a set of candidate genes with potential or known roles in atrial septation. For example, we observed that expression of *Gata6*, required for inflow tract development and atrial septation (Tian et al., 2010), was *Tbx5* dependent in the pSHF but not the heart, suggesting that *Gata6* may play its required role in the pSHF. *Tbx5* has also been shown to regulate cell proliferation in several developmental contexts including the vertebrate heart (Goetz et al., 2006; Hatcher et al., 2001). We observed that *Tbx5* dependent expression of multiple cell-cycle genes controlling progression through M and G1 phases in the pSHF but not the heart, and identified *Cdk6* as a direct *Tbx5* target. *Cdk6* is not required for cell-cycle progression, but instead potentates cell-cycle progress, often in response to signaling (reviewed in Kozar and Sicinski, 2005). Our data support a model that *Tbx5* is not part of the core cell-cycle transcriptional kernel, but is able to engage it in the pSHF to enhance cyclin-D kinase and other cell-cycle gene expression to promote cell-cycle progression.

Tbx5 Acts Upstream of and Parallel to *Hh*-Signaling in Atrial Septation

Tbx5-dependent molecular pathways required for atrial septation remained unknown despite the previous identification of several *Tbx5* transcriptional targets in the heart (Bruneau, 2003; Bruneau et al., 2001; Mori et al., 2006). We provide genetic and molecular evidence that *Tbx5* acts upstream and in parallel to *Hh*-signaling in atrial septation. The genetic observation that constitutive *Hh* signaling can rescue *Tbx5* removal in the pSHF suggests that *Hh* signaling is sufficient to activate an atrial septation gene regulatory network (GRN) (Davidson and Erwin, 2006). This epistasis experiment (Figure 5) placed *Tbx5* upstream

and/or in parallel to *Hh*-signaling, and we discovered molecular support for both possibilities. *Tbx5* is required for pSHF expression of genes required for normal *Hh*-signaling (*Gli1*, *Ptch1*, *Gas1*) (Figure 6A) and *Tbx5* directly activated *Gas1* transcription (Figure 6B). We concluded that *Tbx5* potentiated *Hh*-signaling. However, the modest scale of these effects suggested that *Tbx5* was not absolutely required for pSHF *Hh*-signaling and implied that *Tbx5* also acted in an *Hh*-independent pathway (Figure 6L). A molecular link to a parallel pathway was identified in *Osr1*, a direct *Tbx5* downstream target required for atrial septation (Figure 6).

These observations demonstrate that *Tbx5* acts both upstream and in parallel to *Hh*-signaling during inflow morphogenesis. The molecular findings are consistent with the broader expression of *Tbx5* in the pSHF than *Gli1* (Figure 1) and the more severe inflow phenotype of *Tbx5* (Bruneau et al., 2001) compared to *Shh* knockout mice (Washington Smoak et al., 2005). The broader role for *Tbx5* in cardiac inflow development, upstream and parallel action of *Tbx5* with respect to *Hh* signaling, and capacity of *Hh*-signaling to autonomously activate an atrial septation GRN suggest a model for the molecular control of atrial septation (Figure 6): that *Tbx5* establishes a progenitor field and promotes *Hh*-signaling, which then selects progenitors specific for the atrial septum (Figures 6M and 6N). This work generates a working model for understanding the molecular ontogeny of human ASDs.

Experimental Procedures

Mouse Lines

Mice were a mixed *B6/129/SvEv* background. $Tbx5^{-/+}$, $Tbx5^{fl/+}$, $Gli1^{CreERT2/+}$, $Tie2^{Cre/+}$, the $TnT^{Cre/+}$ and the $Mef2C^{Cre/+}$ mouse lines have been reported (Bruneau et al., 2001; Ahn and Joyner, 2004; Jiao et al., 2003; Kisanuki et al., 2001; Verzi et al., 2005). Smo^{fl}, $Smo\text{-}M2^{fl/fl}$, and $Shh^{-/+}$ mice were obtained from The Jackson Laboratory. Mouse experiments were completed according to a protocol reviewed and approved by the Institutional Animal Care and Use Committee of the University of Chicago, in compliance with the USA Public Health Service Policy on Humane Care and Use of Laboratory Animals.

Microdissection of pSHF and RNA Extraction

Embryos were dissected above the outflow tract and below the inflow tract to obtain a thoracic section including the heart. The neural tube was removed by cutting through the foregut. Cutting between the outflow and inflow tracts separated the pSHF and aSHF. The heart, aSHF, and pSHF were collected separately in RNA-later.

In Situ Hybridization

In situ hybridization was performed as described in (Moorman et al., 2001). Specifically, sense and antisense probes were generated using a digoxigenin (DIG) RNA labeling kit (Roche). Probes were hybridized overnight at 65°C onto E9.5 or E10.5 embryo for both whole mount and section in situ hybridization. DIG-labeled probes were detected by anti-digoxin-AP Fab fragments (Roche) and precipitated by BM purple AP substrate (Roche).

Real-Time PCR

Reverse transcription reaction was performed using a SuperScript III Reverse Transcriptase kit from Invitrogen. Real-time PCR was performed using a POWER SYBER Green PCR mater mix from Applied Biosystems.

Microarray Analysis

Three independent pools of RNA from each biological group were chosen for cRNA amplification and Cyanine-3 labeling using Agilent Quick Amp Labeling kit. Samples were profiled on Agilent Mouse Whole Genome Arrays. One pool was discarded from analysis because of failure to Raw intensity data was normalized using Agilent's Feature extraction software. Data quality was analyzed by assessing data distributions and Q-Q plots between replicates. R statistical package SAM was used to detect differential expressed genes and package GSA was used for gene set enrichment analysis (Tusher et al., 2001; Efron and Tibshirani, 2001).

Immunohistochemistry

Embryos at E9.5 were stained with X-gal (Hoffmann et al., 2009) and sectioned serially at 6 μm. For BrdU incorporation, pregnant mice were given 150 μl BrdU solution at E9.0 with two doses, 3 hr and 6 hr before sacrifice, respectively. The BrdU staining was performed using a BrdU In Situ detection kit (BD Pharmingen). For TUNNEL staining, an ApopTag plus peroxidase In Situ apoptosis detection kit was used (Chemicon). A rabbit anti-mouse p-Histone-H3 (ser10) (Abcam) and an Alexa Fluor 488 goat anti-rabbit IgG (Invitrogen) were used for cell-cycle staining.

Dual Luciferase Reporter Assay

Amplified promoter regions are noted in the results text was cloned into pGL3 Basic vector (Promega) modified to include a minimal TA promoter. *Tbx5* was cloned from a mouse atrial cDNA library into pcDNA3.1 Hygro (Invitrogen). Transient transfections were performed in HEK293T cells using FuGene HD (Promega) according to the manufacturer's instructions. Total cell lysates were prepared 48 hr posttransfection and luciferase activity was assessed using the Promega Dual Luciferase Reporter kit (Promega) according to the manufacturer's protocol.

Chromatin Immunoprecipitation

Anti-protein G Dynabeads (Invitrogen) were prebound overnight to an anti-*Tbx5* antibody (Santa Cruz). Fifty E10 wild-type *CD-1* embryos were isolated in cold PBS with protease inhibitor, and the SHF was microdissected. Tissues were crosslinked in 1.8% formaldehyde solution for 10 min, lysed, sonicated, and incubated with beads overnight. Beads were magnetically precipitated and washed. DNA was eluted from beads using 1% SDS/0.1 M $NaHCO_3$, de-crosslinked with 0.2 M NaCl at 65 centi-degrees and isolated using a PCR clean up kit (QIAGEN). Enrichment was assayed by SYBR green qPCR (Applied Biosystems).

Supplementary Material

Refer to Web version on PubMed Central for supplementary material.

Acknowledgments

This work was funded by grants from the NIH (R01 HL092153 to I.P.M.), the March of Dimes (I.P.M.), the AHA (I.P.M.), and the Schweppe Foundation (I.P.M.).

References

Ahn S, Joyner AL. Dynamic changes in the response of cells to positive hedgehog signaling during mouse limb patterning. Cell. 2004; 118:505–516. [PubMed: 15315762]

Allen BL, Song JY, Izzi L, Althaus IW, Kang JS, Charron F, Krauss RS, McMahon AP. Overlapping roles and collective requirement for the coreceptors GAS1, CDO, and BOC in SHH pathway function. Dev Cell. 2011; 20:775–787. [PubMed: 21664576]

Anderson RH, Webb S, Brown NA, Lamers W, Moorman A. Development of the heart: (2) Septation of the atriums and ventricles. Heart. 2003; 89:949–958. [PubMed: 12860885]

Barr AR, Kilmartin JV, Gergely F. CDK5RAP2 functions in centrosome to spindle pole attachment and DNA damage response. J Cell Biol. 2010; 189:23–39. [PubMed: 20368616]

Basson CT, Bachinsky DR, Lin RC, Levi T, Elkins JA, Soults J, Grayzel D, Kroumpouzou E, Traill TA, Leblanc-Straceski J, et al. Mutations in human TBX5 [corrected] cause limb and cardiac malformation in Holt-Oram syndrome. Nat Genet. 1997; 15:30–35. [PubMed: 8988165]

Blom NA, Ottenkamp J, Wenink AG, Gittenberger-de Groot AC. Deficiency of the vestibular spine in atrioventricular septal defects in human fetuses with down syndrome. Am J Cardiol. 2003; 91:180–184. [PubMed: 12521631]

Bruneau BG, Logan M, Davis N, Levi T, Tabin CJ, Seidman JG, Seidman CE. Chamber-specific cardiac expression of Tbx5 and heart defects in Holt-Oram syndrome. Dev Biol. 1999; 211:100–108. [PubMed: 10373308]

Bruneau BG. The developing heart and congenital heart defects: a make or break situation. Clin Genet. 2003; 63:252–261. [PubMed: 12702154]

Bruneau BG, Nemer G, Schmitt JP, Charron F, Robitaille L, Caron S, Conner DA, Gessler M, Nemer M, Seidman CE, Seidman JG. A murine model of Holt-Oram syndrome defines roles of the T-box transcription factor Tbx5 in cardiogenesis and disease. Cell. 2001; 106:709–721. [PubMed: 11572777]

Chan FK, Zhang J, Cheng L, Shapiro DN, Winoto A. Identification of human and mouse p19, a novel CDK4 and CDK6 inhibitor with homology to p16ink4. Mol Cell Biol. 1995; 15:2682–2688. [PubMed: 7739548]

Crosio C, Fimia GM, Loury R, Kimura M, Okano Y, Zhou H, Sen S, Allis CD, Sassone-Corsi P. Mitotic phosphorylation of histone H3: spatio-temporal regulation by mammalian Aurora kinases. Mol Cell Biol. 2002; 22:874–885. [PubMed: 11784863]

Davidson EH, Erwin DH. Gene regulatory networks and the evolution of animal body plans. Science. 2006; 311:796–800. [PubMed: 16469913]

Dong Y, Bogdanova A, Habermann B, Zachariae W, Ahringer J. Identification of the C. elegans anaphase promoting complex subunit Cdc26 by phenotypic profiling and functional rescue in yeast. BMC Dev Biol. 2007; 7:19. [PubMed: 17374146]

Efron B, Tibshirani R. On testing the significance of sets of genes. Ann Appl Stat. 2001; 1:107–129.

Garg V, Kathiriya IS, Barnes R, Schluterman MK, King IN, Butler CA, Rothrock CR, Eapen RS, Hirayama-Yamada K, Joo K, et al. GATA4 mutations cause human congenital heart defects and reveal an interaction with TBX5. Nature. 2003; 424:443–447. [PubMed: 12845333]

Goddeeris MM, Rho S, Petiet A, Davenport CL, Johnson GA, Meyers EN, Klingensmith J. Intracardiac septation requires hedgehog-dependent cellular contributions from outside the heart. Development. 2008; 135:1887–1895. [PubMed: 18441277]

Goetz SC, Brown DD, Conlon FL. TBX5 is required for embryonic cardiac cell cycle progression. Development. 2006; 133:2575–2584. [PubMed: 16728474]

Hatcher CJ, Kim MS, Mah CS, Goldstein MM, Wong B, Mikawa T, Basson CT. TBX5 transcription factor regulates cell proliferation during cardiogenesis. Dev Biol. 2001; 230:177–188. [PubMed: 11161571]

He A, Kong SW, Ma Q, Pu WT. Co-occupancy by multiple cardiac transcription factors identifies transcriptional enhancers active in heart. Proc Natl Acad Sci USA. 2011; 108:5632–5637. [PubMed: 21415370]

Hiroi Y, Kudoh S, Monzen K, Ikeda Y, Yazaki Y, Nagai R, Komuro I. Tbx5 associates with Nkx2-5 and synergistically promotes cardiomyocyte differentiation. Nat Genet. 2001; 28:276–280. [PubMed: 11431700]

Hoffmann AD, Peterson MA, Friedland-Little JM, Anderson SA, Moskowitz IP. sonic hedgehog is required in pulmonary endoderm for atrial septation. Development. 2009; 136:1761–1770. [PubMed: 19369393]

Izzi L, Lévesque M, Morin S, Laniel D, Wilkes BC, Mille F, Krauss RS, McMahon AP, Allen BL, Charron F. Boc and Gas1 each form distinct Shh receptor complexes with Ptch1 and are required for Shh-mediated cell proliferation. Dev Cell. 2011; 20:788–801. [PubMed: 21664577]

Jiao K, Kulessa H, Tompkins K, Zhou Y, Batts L, Baldwin HS, Hogan BL. An essential role of Bmp4 in the atrioventricular septation of the mouse heart. Genes Dev. 2003; 17:2362–2367. [PubMed: 12975322]

Joyner AL, Zervas M. Genetic inducible fate mapping in mouse: establishing genetic lineages and defining genetic neuroanatomy in the nervous system. Dev Dyn. 2006; 235:2376–2385. [PubMed: 16871622]

Kasahara H, Bartunkova S, Schinke M, Tanaka M, Izumo S. Cardiac and extracardiac expression of Csx/Nkx2.5 homeodomain protein. Circ Res. 1998; 82:936–946. [PubMed: 9598591]

Kisanuki YY, Hammer RE, Miyazaki J, Williams SC, Richardson JA, Yanagisawa M. Tie2-Cre transgenic mice: a new model for endothelial cell-lineage analysis in vivo. Dev Biol. 2001; 230:230–242. [PubMed: 11161575]

Kozar K, Sicinski P. Cell cycle progression without cyclin D-CDK4 and cyclin D-CDK6 complexes. Cell Cycle. 2005; 4:388–391. [PubMed: 15738651]

Kuo CT, Morrisey EE, Anandappa R, Sigrist K, Lu MM, Parmacek MS, Soudais C, Leiden JM. GATA4 transcription factor is required for ventral morphogenesis and heart tube formation. Genes Dev. 1997; 11:1048–1060. [PubMed: 9136932]

Li QY, Newbury-Ecob RA, Terrett JA, Wilson DI, Curtis AR, Yi CH, Gebuhr T, Bullen PJ, Robson SC, Strachan T, et al. Holt-Oram syndrome is caused by mutations in TBX5, a member of the Brachyury (T) gene family. Nat Genet. 1997; 15:21–29. [PubMed: 8988164]

Malumbres M, Barbacid M. Mammalian cyclin-dependent kinases. Trends Biochem Sci. 2005; 30:630–641. [PubMed: 16236519]

Mao J, Ligon KL, Rakhlin EY, Thayer SP, Bronson RT, Rowitch D, McMahon AP. A novel somatic mouse model to survey tumorigenic potential applied to the Hedgehog pathway. Cancer Res. 2006; 66:10171–10178. [PubMed: 17047082]

Mommersteeg MT, Soufan AT, de Lange FJ, van den Hoff MJ, Anderson RH, Christoffels VM, Moorman AF. Two distinct pools of mesenchyme contribute to the development of the atrial septum. Circ Res. 2006; 99:351–353. [PubMed: 16873717]

Moorman AF, Houweling AC, de Boer PA, Christoffels VM. Sensitive nonradioactive detection of mRNA in tissue sections: novel application of the whole-mount in situ hybridization protocol. J Histochem Cytochem. 2001; 49:1–8. [PubMed: 11118473]

Mori AD, Zhu Y, Vahora I, Nieman B, Koshiba-Takeuchi K, Davidson L, Pizard A, Seidman JG, Seidman CE, Chen XJ, et al. Tbx5-dependent rheostatic control of cardiac gene expression and morphogenesis. Dev Biol. 2006; 297:566–586. [PubMed: 16870172]

Nadeau M, Georges RO, Laforest B, Yamak A, Lefebvre C, Beauregard J, Paradis P, Bruneau BG, Andelfinger G, Nemer M. An endocardial pathway involving Tbx5, Gata4, and Nos3 required for atrial septum formation. Proc Natl Acad Sci USA. 2010; 107:19356–19361. [PubMed: 20974940]

Olson EN. Gene regulatory networks in the evolution and development of the heart. Science. 2006; 313:1922–1927. [PubMed: 17008524]

Pérez-Pérez JM, Serralbo O, Vanstraelen M, GonzÁlez C, Criqui MC, Genschik P, Kondorosi E, Scheres B. Specialization of CDC27 function in the Arabidopsis thaliana anaphase-promoting complex (APC/C). Plant J. 2008; 53:78–89. [PubMed: 17944809]

Plageman TF Jr, Yutzey KE. Microarray analysis of Tbx5-induced genes expressed in the developing heart. Dev Dyn. 2006; 235:2868–2880. [PubMed: 16894625]

Rao CV, Yamada HY, Yao Y, Dai W. Enhanced genomic instabilities caused by deregulated microtubule dynamics and chromosome segregation: a perspective from genetic studies in mice. Carcinogenesis. 2009; 30:1469–1474. [PubMed: 19372138]

Schott JJ, Benson DW, Basson CT, Pease W, Silberbach GM, Moak JP, Maron BJ, Seidman CE, Seidman JG. Congenital heart disease caused by mutations in the transcription factor NKX2-5. Science. 1998; 281:108–111. [PubMed: 9651244]

Soriano P. Generalized lacZ expression with the ROSA26 Cre reporter strain. Nat Genet. 1999; 21:70–71. [PubMed: 9916792]

Snarr BS, O'Neal JL, Chintalapudi MR, Wirrig EE, Phelps AL, Kubalak SW, Wessels A. Isl1 expression at the venous pole identifies a novel role for the second heart field in cardiac development. Circ Res. 2007a; 101:971–974. [PubMed: 17947796]

Snarr BS, Wirrig EE, Phelps AL, Trusk TC, Wessels A. A spatiotemporal evaluation of the contribution of the dorsal mesenchymal protrusion to cardiac development. Dev Dyn. 2007b; 236:1287–1294. [PubMed: 17265457]

Takeuchi JK, Bruneau BG. Directed transdifferentiation of mouse mesoderm to heart tissue by defined factors. Nature. 2009; 459:708–711. [PubMed: 19396158]

Tian Y, Cohen ED, Morrisey EE. The importance of Wnt signaling in cardiovascular development. Pediatr Cardiol. 2010; 31:342–348. [PubMed: 19967349]

Tusher VG, Tibshirani R, Chu G. Significance analysis of microarrays applied to the ionizing radiation response. Proc Natl Acad Sci USA. 2001; 98:5116–5121. [PubMed: 11309499]

Ueyama T, Kasahara H, Ishiwata T, Nie Q, Izumo S. Myocardin expression is regulated by Nkx2.5, and its function is required for cardiomyogenesis. Mol Cell Biol. 2003; 23:9222–9232. [PubMed: 14645532]

Vagnarelli P, Hudson DF, Ribeiro SA, Trinkle-Mulcahy L, Spence JM, Lai F, Farr CJ, Lamond AI, Earnshaw WC. Condensin and Repo-Man-PP1 co-operate in the regulation of chromosome architecture during mitosis. Nat Cell Biol. 2006; 8:1133–1142. [PubMed: 16998479]

Verzi MP, McCulley DJ, De Val S, Dodou E, Black BL. The right ventricle, outflow tract, and ventricular septum comprise a restricted expression domain within the secondary/anterior heart field. Dev Biol. 2005; 287:134–145. [PubMed: 16188249]

Wang Q, Lan Y, Cho ES, Maltby KM, Jiang R. Odd-skipped related 1 (Odd 1) is an essential regulator of heart and urogenital development. Dev Biol. 2005; 288:582–594. [PubMed: 16223478]

Washington Smoak I, Byrd NA, Abu-Issa R, Goddeeris MM, Anderson R, Morris J, Yamamura K, Klingensmith J, Meyers EN. Sonic hedgehog is required for cardiac outflow tract and neural crest cell development. Dev Biol. 2005; 283:357–372. [PubMed: 15936751]

Wehman AM, Staub W, Baier H. The anaphase-promoting complex is required in both dividing and quiescent cells during zebrafish development. Dev Biol. 2007; 303:144–156. [PubMed: 17141209]

Wessels A, Anderson RH, Markwald RR, Webb S, Brown NA, Viragh S, Moorman AF, Lamers WH. Atrial development in the human heart: an immunohistochemical study with emphasis on the role of mesenchymal tissues. Anat Rec. 2000; 259:288–300. [PubMed: 10861362]

Xiong Y, Zhang H, Beach D. D type cyclins associate with multiple protein kinases and the DNA replication and repair factor PCNA. Cell. 1992; 71:505–514. [PubMed: 1358458]

Zhang XM, Ramalho-Santos M, McMahon AP. Smoothened mutants reveal redundant roles for Shh and Ihh signaling including regulation of L/R asymmetry by the mouse node. Cell. 2001; 105:781–792. [PubMed: 11440720]

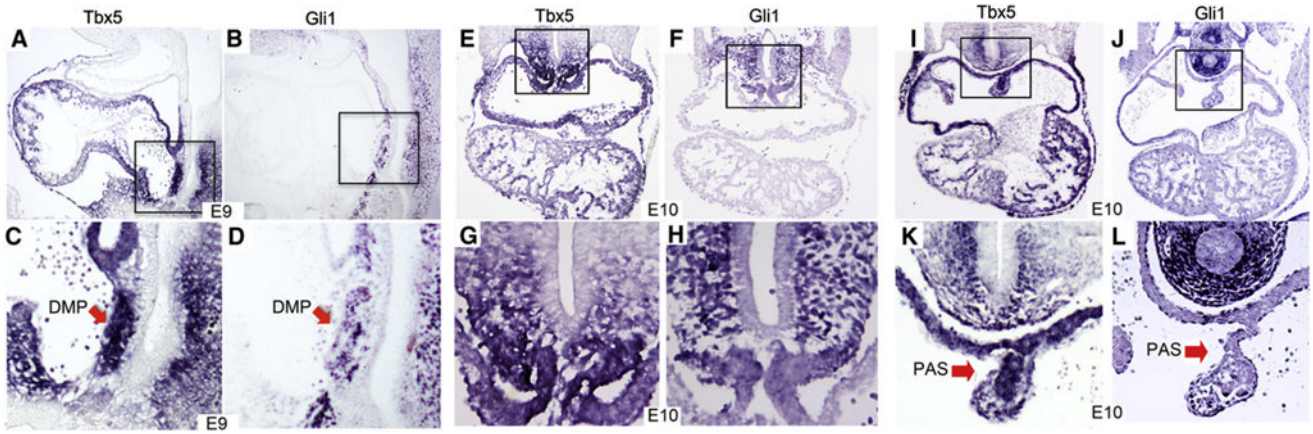

Figure 1. *Tbx5* Is Expressed in the Posterior Second Heart Field

Expression of *Tbx5* and *Gli1* analyzed by in situ hybridization on *wild-type* mouse embryos in sagittal sections at E9.0 (A–D) and transverse sections at E10.0 (E–L). *Tbx5* (C and G) and *Gli1* (D and H) were both expressed in the DMP and the splanchnic mesoderm. *Tbx5* (I and K) but not *Gli1* (J and L) was also expressed in the heart. Magnification: (A), (B), (E), (F), (I), (J) = 100×; (C), (D), (G), (H), (K), (L) = 400×.

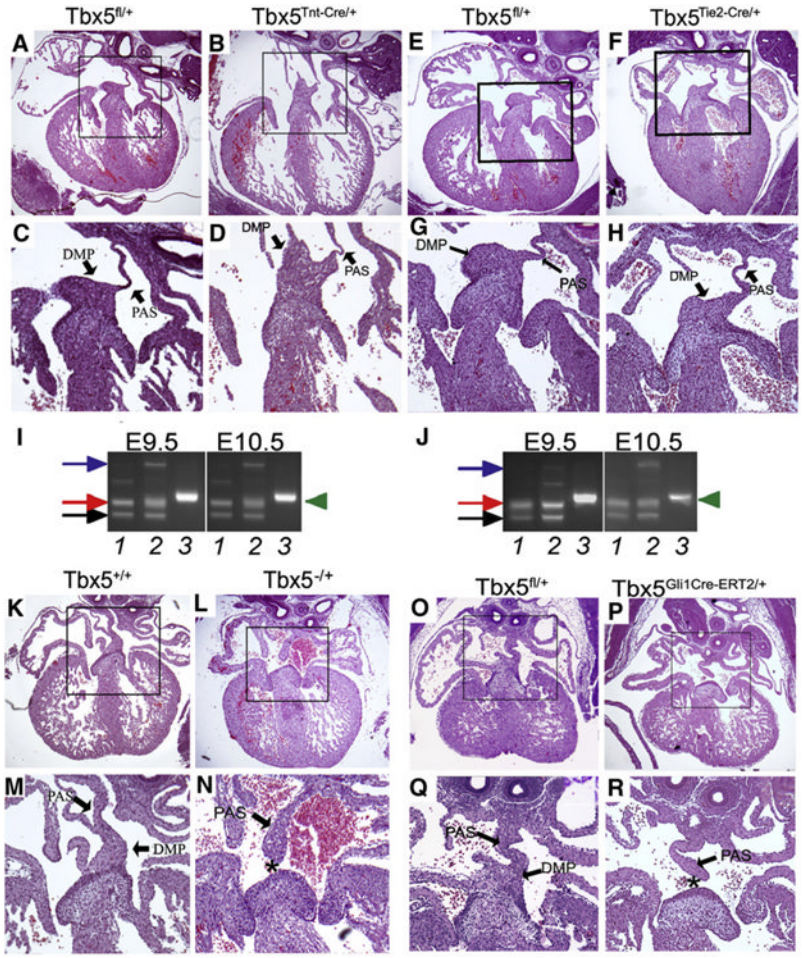

Figure 2. *Tbx5* Is Not Required in the Myocardium or Endocardium but Is Required in SHF *Hh*-Receiving Cells for Atrial Septation

(A–H) Analysis of atrial septation in myocardial or endocardial *Tbx5* mutant embryos. Atrial septation was normal in $Tbx5^{fll/+}$ (A, C, E, G; 7/7), $Tbx5^{Tnt\text{-}Cre/+}$ embryos (B, D; 7/7; p = 1), and $Tbx5^{Tie2\text{-}Cre/+}$ (F,H; 7/7; p = 1) embryos at E13.5.

(I and J) *Cre*-dependent somatic recombination of conditional *Tbx5* locus. At both E9.5 and E10.5, hearts from $Tbx5^{Tnt\text{-}Cre/+}$ (I) and $Tbx5^{Tie2\text{-}Cre/+}$ (J) demonstrated a *Tbx5* null allele (blue arrow, 480 bp band) and *Cre* expression (green arrow head, 220 bp band) in the heart (lane 2, 3) but not the tail (lane 1). Both the heart and tail DNA showed *Tbx5 wild-type* (black arrow: 158 bp band) and *Tbx5-flox* (red arrow: 198 bp band) alleles.

(K–R) Atrial septal defects in germline and SHF *Tbx5* mutant embryos. Primum ASDs were observed in 40% of $Tbx5^{-/+}$ embryos, consistent with previous reports (Bruneau et al., 2001), (L and N) (5/12; p = 0.0466) and 40% of $Tbx5^{Gli1Cre\text{-}ERT2/+}$ embryos (P and R) (5/12) compared to 0% of $Tbx5^{fl/+}$ embryos (O and Q) (0/7; p = 0.0466) at E13.5 in transverse sections. Magnification: (A), (B), (E), (F), (K), (L), (O), (P) = 40×; (C), (D), (G), (H), (M), (N), (Q), (R) = 100×.

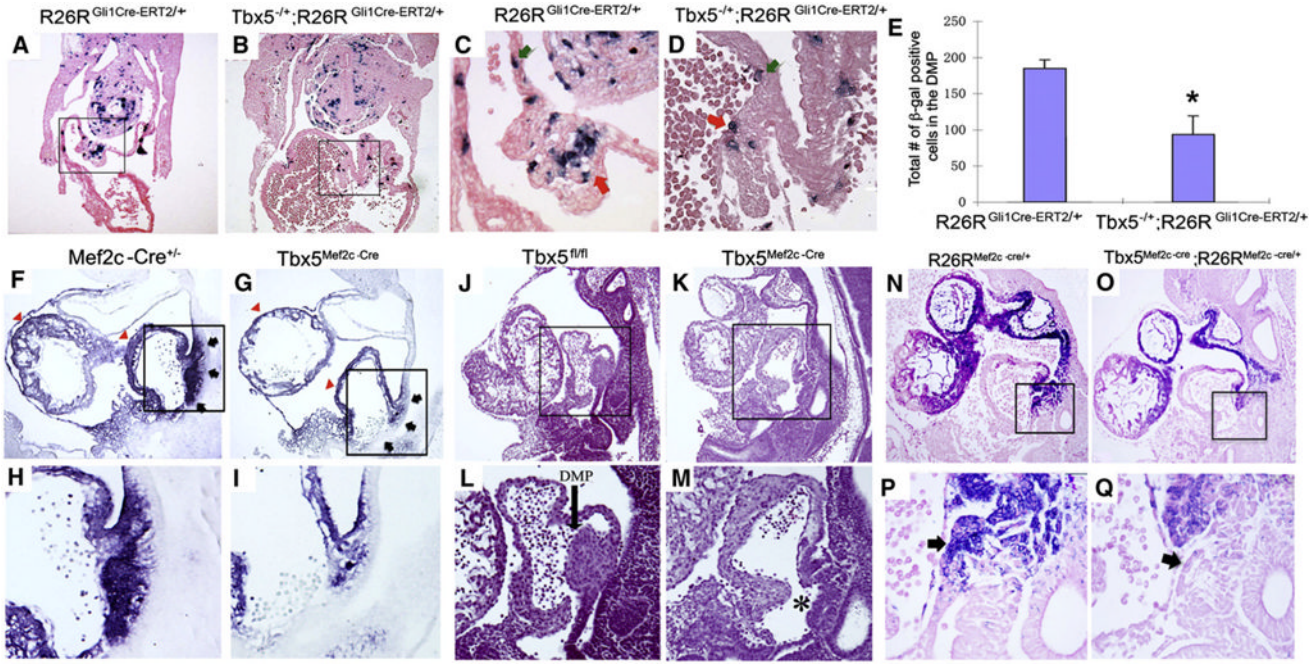

Figure 3. *Tbx5* Is Required in SHF *Hh*-Receiving Cells for Atrial Septation

(A–E) *Hh*-receiving cardiac fate map in *Tbx5* mutant embryos. *Hh*-receiving cells were marked by β-galactosidase expression in $R26R^{Gli1Cre\text{-}ERT2/+}$ embryos at E7.5 and E8.5 by tamoxifen administration and analyzed by at E10.5. All β-galactosidase positive cells in the dorsal mesenchymal protrusion (DMP) (red arrows in C and D) were counted. Significantly fewer β-gal positive DMP cells were present in $Tbx5^{-/+}$; $R26R^{Gli1Cre\text{-}ERT2/+}$ embryos (187.4 ±11.5) Data are presented as mean ± SEM, n = 3–4. (B and D) compared to $R26R^{Gli1Cre\text{-}ERT2/+}$ embryos (92.4 ± 24.1, p = 0.0265) (A and C).

(F–I) *Tbx5* expression in SHF *Tbx5* mutant embryos. *Tbx5* expression is extinguished specifically in the DMP and SHF of $Tbx5^{Mef2c\text{-}Cre}$ but not $Mef2c^{Cre/+}$ embryos at E9.5 by in situ hybridization. Myocardial *Tbx5* expression is maintained in both genotypes (F and G red arrows).

(J–M) SHF *Tbx5* expression is required for DMP development. The DMP was a well-defined structure in $Tbx5^{fl/fl}$ embryos (L, black arrow; 5/5) but absent in $Tbx5^{Mef2c\text{-}Cre}$ embryos (K and M; 0/5; p = 0.0005).

(N–Q) Absence of SHF fate map in *Tbx5* SHF mutant embryos. β-galactosidase expressing cells are absent from the pSHF including the DMP region in $Tbx5^{Mef2c\text{-}Cre}$;$R26R^{Mef2c\text{-}Cre/+}$ embryos (Q, black arrow) but present in control $R26R^{Mef2c\text{-}Cre/+}$ embryos (P, black arrow) at E9.5. β-galactosidase positive cells are observed in the anterior SHF, outflow tract, and right ventricles in both genotypes (N and P versus O and Q). Data are presented as mean ± SEM, n = 3–4. Magnification: (A), (B), (F), (G), (J), (K), (N), (O) = 100×; (C), (D), (H), (I), (L), (M), (P), (Q) = 400×.

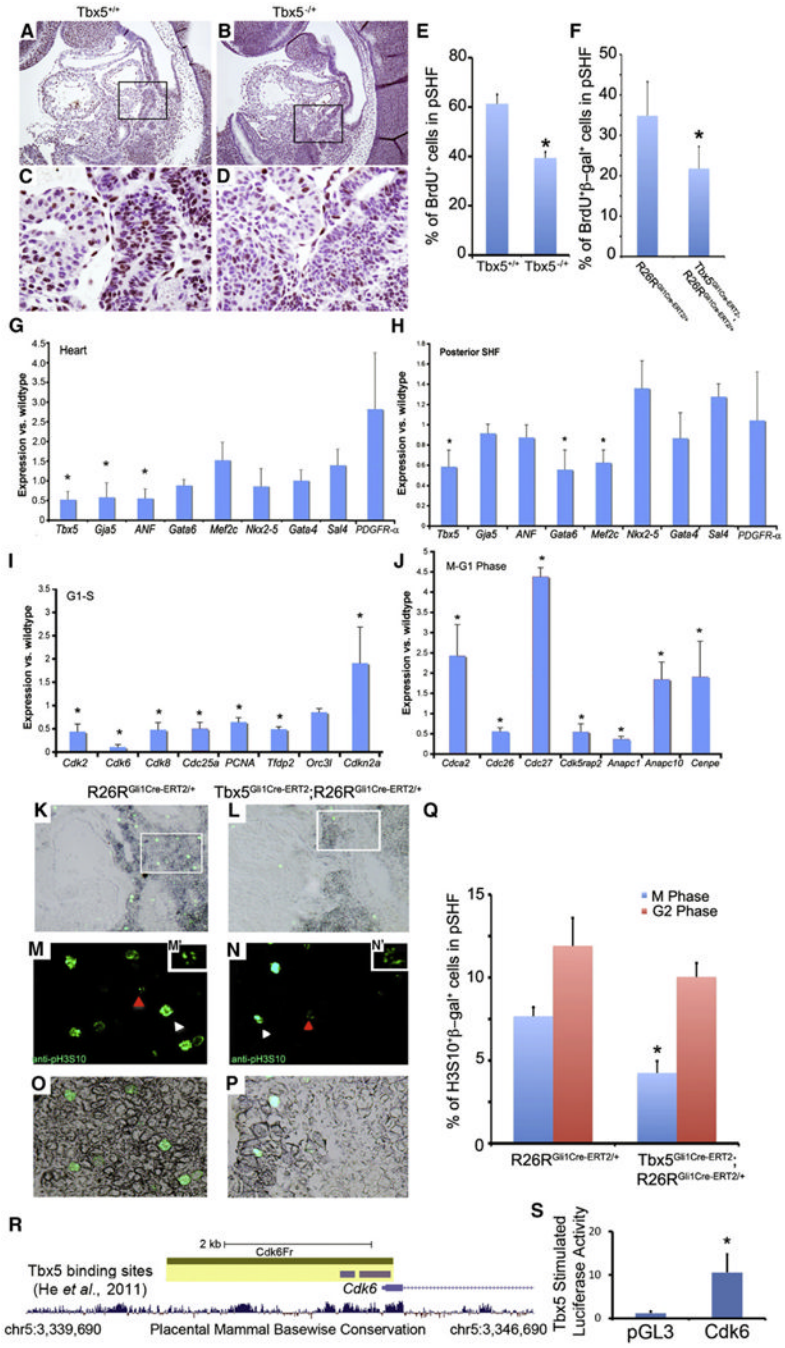

Figure 4. *Tbx5* Is Required for Cell-Cycle Progress of Posterior SHF Cardiac Progenitors

(A–F) PSHF proliferation requires *Tbx5*. Fewer pSHF BrdU incorporated cells were observed in $Tbx5^{-/+}$ (B, D, E) than wild-type embryos (A, C, E) (61.4% ± 4.3% versus 34% ± 5.7%, p = 0.001). Fewer BrdU and *Hh*-receiving β-galactosidase pSHF comarked cells were observed in $Tbx5^{Gli1Cre\text{-}ERT2};R26R^{Gli1Cre\text{-}ERT2/+}$ embryos than in $R26R^{Gli1Cre\text{-}ERT2/+}$ embryos (34.9% ± 8.4% versus 21.6% ± 5.6%, p = 0.0492). Data are presented as mean ± SEM, n = 3–4.

(G–J) Distinct *Tbx5*-dependent transcripts in the pSHF and heart at E9.5 by real-time PCR. *Tbx5* was downregulated in the heart and pSHF (G and H). *Nppa* and *Gja5* were

downregulated in the heart but not the pSHF (G and H). *Gata6* and *Mef2c* were downregulated in the posterior SHF but not in the heart. (I and J) Genes that promote G1-S progress (*Cdk2*, *Cdk6*, *Cdk25a*, *PCNA*, *Tfbp2*) were downregulated whereas a gene that represses G1-S progress (*Cdkn2a)* was upregulated. Data are presented as mean ± SEM, n = 3–4.

(K–Q) *Tbx5* is required for cell-cycle progression in *Hh*-receiving pSHF cells. Significantly fewer β-galactosidase marked pSHF *Hh*-receiving cells were observed in M-phase by anti-Histone-H3 (H3S10) immunohistochemistry in $R26R^{Gli1Cre\text{-}ERT2/+}$; $Tbx5^{Gli1Cre\text{-}ERT2}$ embryos than in $R26R^{Gli1Cre\text{-}ERT2/+}$ embryos (N and M, white arrowheads mark cells in mitosis diffuse nuclear staining) (7.73 ± 0.51% versus 4.25 ± 0.71%, p = 0.0037). There was no difference in the number of late G2 cells (M and N, red arrowhead marking cell in G2 phase with punctate nuclear staining) (15.31 ±2.23% versus 14.60± 1.94%, p = 0.9237). (Q) Quantification of H3S10 and β-galactosidase costained cells in the pSHF and DMP region. Magnification: (A), (B), (K), (L) = 100×; (C), (D), (M)–(P) = 400×.

(R) Schematic of mouse *Cdk6* including *Tbx5* binding region (He et al., 2011) adjacent to *Cdk6* promoter and cloned genomic fragment tested for *Tbx5*-dependent expression (green bar). Data are presented as mean ± SEM, n = 3–4.

(S) *Tbx5* significantly stimulated firefly luciferase expression from the *Cdk6* promoter region compared to pGL3-vector control (10.55 ± 4.27 versus 1.28 ± 0.49, p < 0.009). Data are presented as mean ±SEM, n = 3.

See also Figure S1 and Tables S1 and S2.

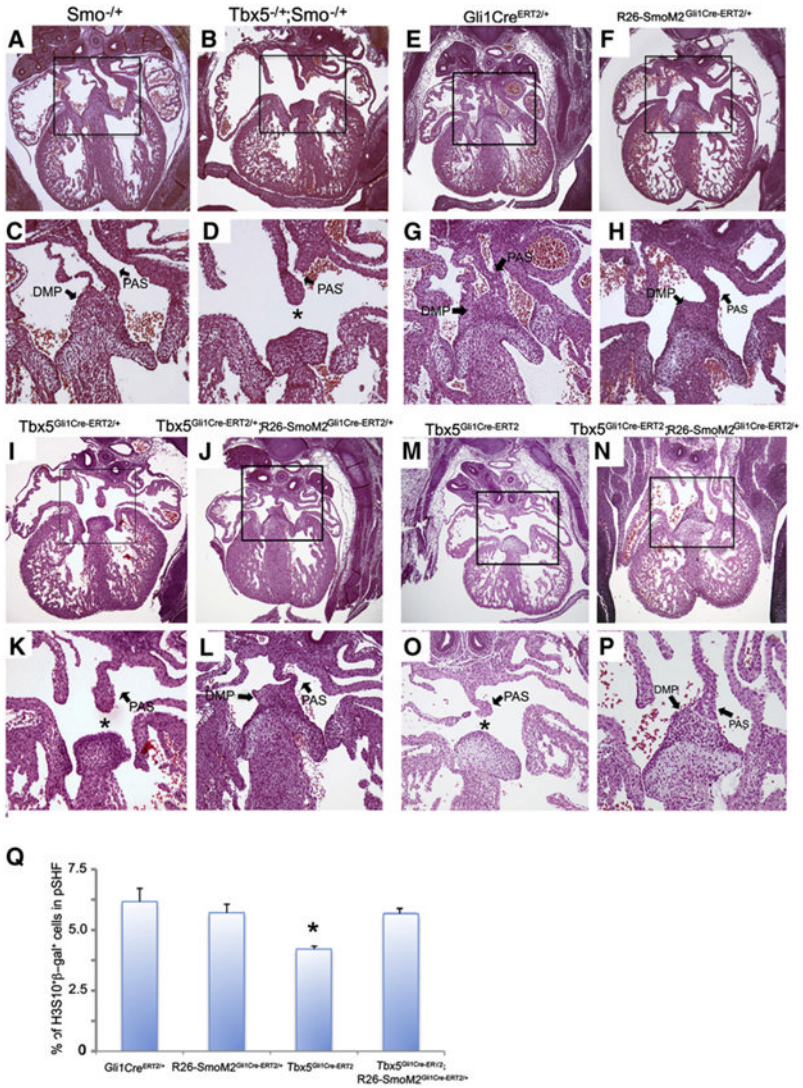

Figure 5. *Hh*-Signaling Is Epistatic to *Tbx5* in Atrial Septation

(A–D) Genetic interaction between *Tbx5* and *Smo* in atrial septation. $Tbx5^{-/+}$; $Smo^{-/+}$ embryos (A and D) demonstrated significantly more ASDs (7/8) than $Tbx5^{-/+}$ embryos (5/12; p = 0.0404) or $Smo^{-/+}$ embryos (A and C)(0/7; p = 0.0007) at E14.5.

(E–P) Rescue of ASDs in *Tbx5* SHF mutant embryos by constitutive *Hh*-signaling. Primum ASDs were observed in 40% of $Tbx5^{Gli1Cre\text{-}ERT2/+}$ (I and k; 5/12) but 0% of *R26-SmoM2* $^{Gli1Cre\text{-}ERT2/+}$;*Tbx5* $^{Gli1Cre\text{-}ERT2/+}$ embryos (J and L) (p = 0.0098). Primum ASDs were observed in 100% of $Tbx5^{Gli1Cre\text{-}ERT2}$ (M and O; 5/5) but 20% of *R26-SmoM2* $^{Gli1Cre\text{-}ERT2/+}$; *Tbx5* $^{Gli1Cre\text{-}ERT2}$ embryos (N and P) (1/5; p = 0.0109). No heart defects were observed in $Gli1Cre^{ERT2/+}$ or *R26-SmoM2* $^{Gli1Cre\text{-}ERT2/+}$ embryos.

(Q) The decreased percentage of phosphorylated H3-histone positive β-galactosidase positive pSHF cells in *Tbx5* $^{Gli1\ Cre\text{-}ERT2}$ *R26R* $^{Gli1Cre\text{-}ERT2/+}$ embryos compared to $Gli1Cre^{ERT2/+}$ *or R26-SmoM2*$^{Gli1Cre\text{-}ERT2/+}$, $R26R^{Gli1Cre\text{-}ERT2/+}$ embryos was normalized in *R26-SmM2* $^{Gli1Cre\text{-}ERT2/+}$ *Tbx5* $^{Gli1Cre\text{-}ERT2}$ *R26R* $^{Gli1Cre\text{-}ERT2/+}$ embryos at E9.5. Data are presented as mean ± SEM, n = 3–4.

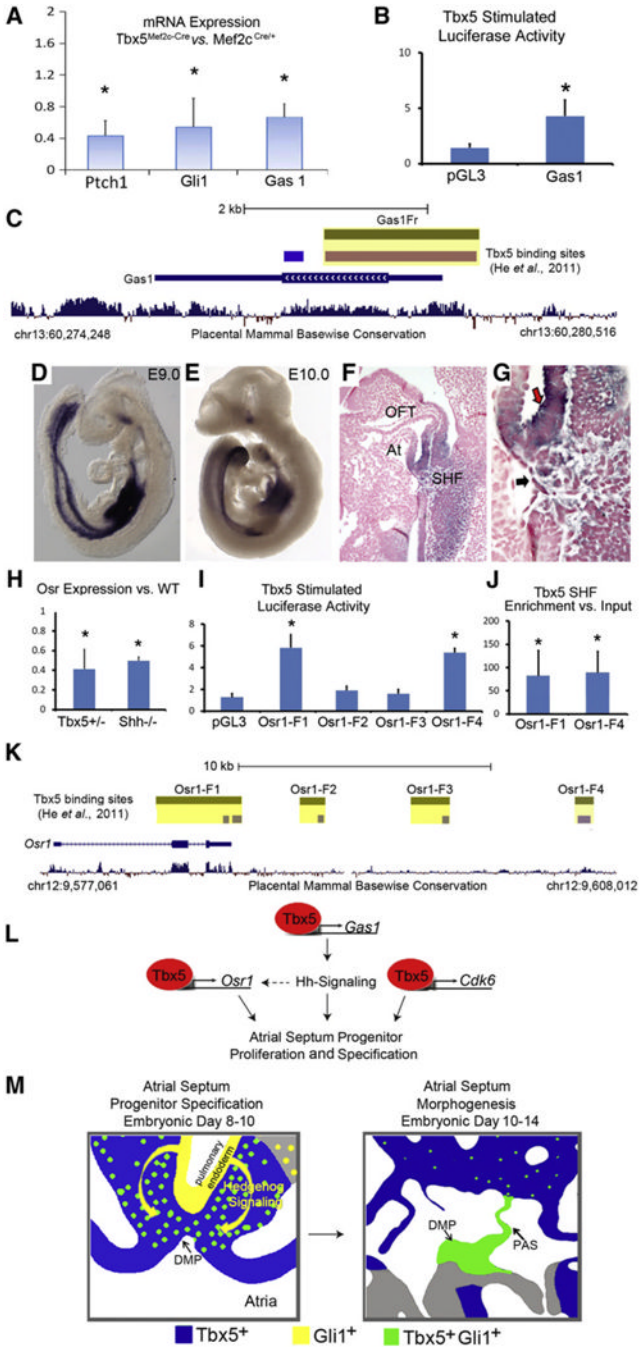

Figure 6. *Tbx5* Act Upstream and Parallel to *Hh-signaling* in Atrial Septation

(A) Decreased expression of *Hh*-dependent genes in the SHF of *Tbx5* mutant embryos. *Ptch*, *Gli1*, and *Gas1* expression were significantly decreased in $Tbx5^{-/+}$ embryos at E9.5 by real-time PCR. Data are presented as mean ± SEM, n = 3–4.

(B) *Tbx5* significantly stimulated firefly luciferase expression from the *Gas1* promoter region compared to pGL3-vector control (4.288 ± 1.43 versus 1.424 ± 0.357, $p < 0.05$). Data are presented as mean ± SEM, n = 3.

(C) Schematic of mouse *Gas1* including *Tbx5* binding region (He et al., 2011) adjacent to *Gas1* promoter and the cloned genomic fragment tested for *Tbx5*-dependent expression in vitro (green bar). See also Table S2.

(D–G) Expression of *Osr1* analyzed by in situ hybridization on wild-type mouse embryos by whole mount at E9 (D) and E10 (E) and sagittal sections at E9.5 (F and G). *Osr1* was expressed robustly in the pSHF and DMP (black arrow, DMP reflection) and splanchnic mesothelium (red arrow, dorsal mesocardium). At, atrium; OFT, outflow tract; SHF, second heart field. Magnification: (D) and (E) = 100×; (F) and (G) = 400 ×.

(H) Expression of *Osr1* is decreased in pSHF of $Tbx5^{-/+}$ (fold change, 0.41 ± 0.2, $p < 0.05$) and $Shh^{-/-}$ embryos 0.5 ± 0.04, $p < 0.05$) compared to wild-type embryos at E9.5 by real-time-PCR. Data are presented as mean ± SEM, n = 3.

(I) *Tbx5* significantly stimulated firefly luciferase expression from *Osr1* genomic fragments Osr1-F1 (5.82 ± 1.42; $p = 0.0009$) and Osr1-F4 (5.6 ± 1.02; $p = 0.0009$) compared to pGL3 empty vector (1.28 ± 0.49). *Tbx5* did not stimulate expression from *Osr1* genomic fragments Osr1-F2 (1.4 ± 0.59; $p = 0.61$; $p = 0.28$) or Osr1-F3 (1.5 ± 0.41). Data are presented as mean ± SEM, n = 3. See also Table S2.

(J) *Tbx5* binds to *Tbx5* responsive *Osr1* genomic fragment in the SHF by ChIP-PCR. The *Tbx5*-responsive DNA fragments were immunoprecipated by *Tbx5* antibody and were amplified by real-time PCR. Osr1-F1 (98.14 ± 45.72) and Osr1-F4 (82.54 ± 54.06) were significantly enriched compared to input DNA. Data are presented as mean ± SEM, n = 3. See also Table S2.

(K) Schematic of mouse *Osr1* including *Tbx5* binding region (He et al., 2011) adjacent to *Osr1* and the cloned genomic fragments Osr1-F1-F4 tested for Tbx5-dependent expression *in-vitro* (green bar). See also Table S2.

(L) Model of *Tbx5* transcriptional regulation in atrial septation. *Tbx5* acts upstream of *Hh*-signaling, directly activating *Gas1* expression. *Tbx5* acts parallel to *Hh*-signaling, directly activating *Osr1* expression. *Tbx5* also directly activates *Cdk6* in regulating atrial progenitor proliferation.

(M and N) Model for combinatorial role of *Tbx5* and *Hh*-signaling in atrial septation. *Tbx5* promotes proliferation of pSHF inflow cardiac progenitors and *Hh*-signaling. PSHF *Hh*-signal receiving $Tbx5^{+}Gli1^{+}$ cells are specified as atrial septum progenitors and generate the atrial septum.

Table 1
Incidence of ASDs in *Tbx5* Mutant Embryos

Genotype	ASD	Total	p Value (χ^2 Test)	
Conditional Haploinsufficiency of *Tbx5*				
Tbx5 $^{-/+}$	5	12	*Tbx5*$^{-/+}$ *(5/12): Tbx5*$^{+/+}$*(0/7)*	p = 0.0466
Tbx5$^{Tnt\text{-}Cre/+}$	0	7	*Tbx5*$^{Tnt\text{-}Cre/+}$*(0/7): Tbx5*$^{-/+}$ *(5/12)*	p = 0.0466
Tbx5$^{Tie2\text{-}Cre/+}$	0	7	*Tbx5*$^{Tnt\text{-}Cre/+}$*(0/7): Tbx5*$^{-/+}$ *(5/12)*	p = 0.0466
Tbx5$^{Gli1cre\text{-}ERT2/+}$	5	12	*Tbx5*$^{Gli1cre\text{-}ERT2/+}$*(5/12): Tbx5*$^{fl/+}$*(0/7)*	p = 0.0466
			Tbx5$^{Gli1cre\text{-}ERT2/+}$*(5/12):Tbx5*$^{-/+}$*(5/12)*	p=1
Tbx5$^{-/+}$*;Gli1Cre*$^{ERT2/+}$	5	11	*Tbx5*$^{-/+}$*;Gli1Cre*$^{ERT2/+}$*(5/11): Tbx5*$^{-/+}$ *(5/12)*	p = 0.8547
Tbx5$^{Mef2c\text{-}Cre/+}$	0	7	*Tbx5*$^{Mef2c\text{-}Cre/+}$ *(0/7): Tbx5*$^{fl/+}$ *(0/7)*	p=1
Conditional Knockout of *Tbx5* in the SHF				
Tbx5$^{Gli1cre\text{-}ERT2}$	5	5	*Tbx5*$^{Gli1cre\text{-}ERT2}$*(5/5): Tbx5*$^{fl/fl}$*(0/7)*	p = 0.0005
			Tbx5$^{Gli1cre\text{-}ERT2}$*(5/5): Tbx5*$^{Gli1cre\text{-}ERT2/+}$ *(5/11)*	p = 0.0367
Tbx5$^{Mef2c\text{-}Cre}$	5[a]	5[a]	*Tbx5*$^{Mef2c\text{-}Cre}$*(5/5): Tbx5*$^{fl/fl}$*(0/7)*	p = 0.0005[a]
Smo-Tbx5 Compound Mutant Embryos				
Tbx5$^{-/+}$*; Smo*$^{-/+}$	7	8	*Tbx5*$^{-/+}$*; Smo*$^{-/+}$ *(7/8): Tbx5*$^{-/+}$ (5/12)	p = 0.0404
			Tbx5$^{-/+}$*;Smo*$^{-/+}$ *(7/8): Smo*$^{-/+}$ (0/7)	p = 0.0007
Tbx5$^{Gli1cre\text{-}ERT2/+}$*; R26-SmoM2*$^{Gli1cre\text{-}ERT2/+}$	0	11	*Tbx5*$^{Gli1cre\text{-}ERT2/+}$*; R26-SmoM2*$^{Gli1cre\text{-}ERT2/+}$*(0/11)*	p = 0.0109
			Tbx5$^{Gli1cre\text{-}ERT2/+}$*(5/11)*	
Tbx5$^{Gli1cre\text{-}ERT2}$*; R26-SmoM2* $^{Gli1cre\text{-}ERT2/+}$	1	5	*Tbx5*$^{Gli1cre\text{-}ERT2}$*; R26-SmoM2*$^{Gli1cre\text{-}ERT2/+}$ *(1/5)*	p = 0.0098
			Tbx5$^{Gli1cre\text{-}ERT2}$*(5/5)*	

Incidence of ASDs was evaluated in *Tbx5* mutant embryos at E13.5 or E14.5. Significance in ASD incidence between *Tbx5* mutant embryos and littermate controls was analyzed by χ^2 test. ASD, atrial septal defects; DMP, dorsal mesenchymal protrusion; SHF, second heart field.

[a]Embryos were examined at E10.5; severely hypoplastic DMPs were observed in all embryos.